

How does dense phase CO₂ influence the phase behaviour of block copolymers synthesised by dispersion polymerisation?

J. Jennings,^a S. P. Bassett,^a D. Hermida-Merino,^b G. Portale,^b W. Bras,^b L. Knight,^a J. J. Titman,^a T. Higuchi,^c H. Jinnai,^c S. M. Howdle^a

^a *School of Chemistry, University of Nottingham, University Park, Nottingham, NG7 2RD, UK. E-mail: steve.howdle@nottingham.ac.uk; Fax: +0044 115 846 8459; Tel: +44 (0)115 9513486*

^b *DUBBLE@ESRF, Netherlands Organisation for Scientific Research (N.W.O.), CS40220, 38043, Grenoble, Cedex 9, France*

^c *Institute of Multidisciplinary Research for Advanced Materials (IMRAM), Tohoku University, 2-1-1 Katahira, Aoba-ku, Sendai 980-8577, Japan*

Supplementary Information

Experimental

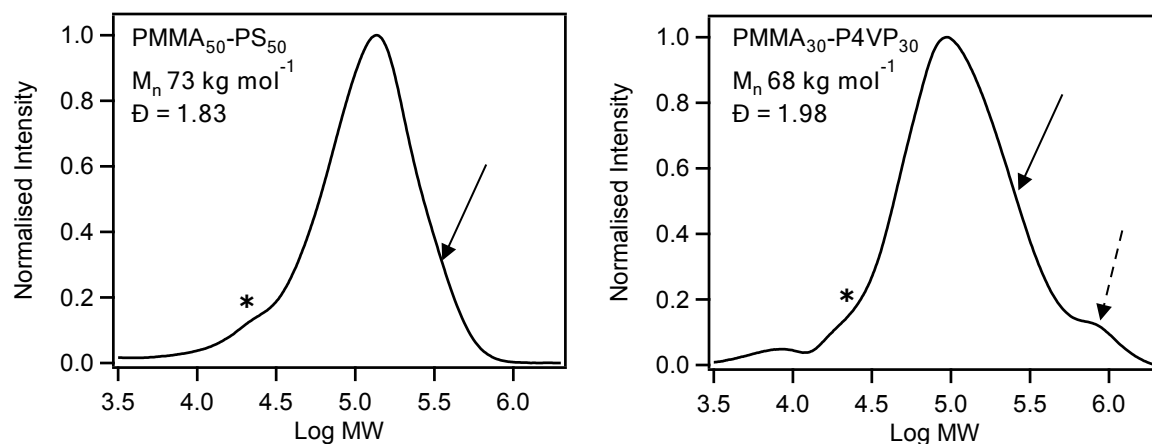
Materials.

S-Dodecyl-S'-(α,α' -dimethyl- α'' -acetic acid)-trithiocarbonate (DATC) was synthesised following literature procedure.¹ α -Azobisisobutyronitrile (AIBN, Wako, 97%) was purified by recrystallizing twice in methanol. Methyl methacrylate (MMA, Fisher, >99%), benzyl methacrylate (BzMA, Alfa Aesar, 98%) and styrene (St, Alfa Aesar, 99%) were purified by eluting through a basic alumina and 4-vinylpyridine (4VP, Alfa Aesar, 96%) was distilled under vacuum prior to use. Poly(dimethylsiloxane monomethyl methacrylate) (PDMS-MA, ABCR, $M_n = 10,000 \text{ g mol}^{-1}$), CDCl₃ (Aldrich), iodine (Fisher), osmium tetroxide (OsO₄, Aldrich) and ruthenium tetroxide (RuO₄, Acros, 0.5% solution in water) were used as received. HPLC grade THF (Fisher), HPLC grade chloroform (Aldrich) and HPLC grade ethanol (Fluka) were used without further purification. Agar 100 resin (Agar Scientific) was used as received, and mixed to target a formulation of medium hardness for embedding samples.

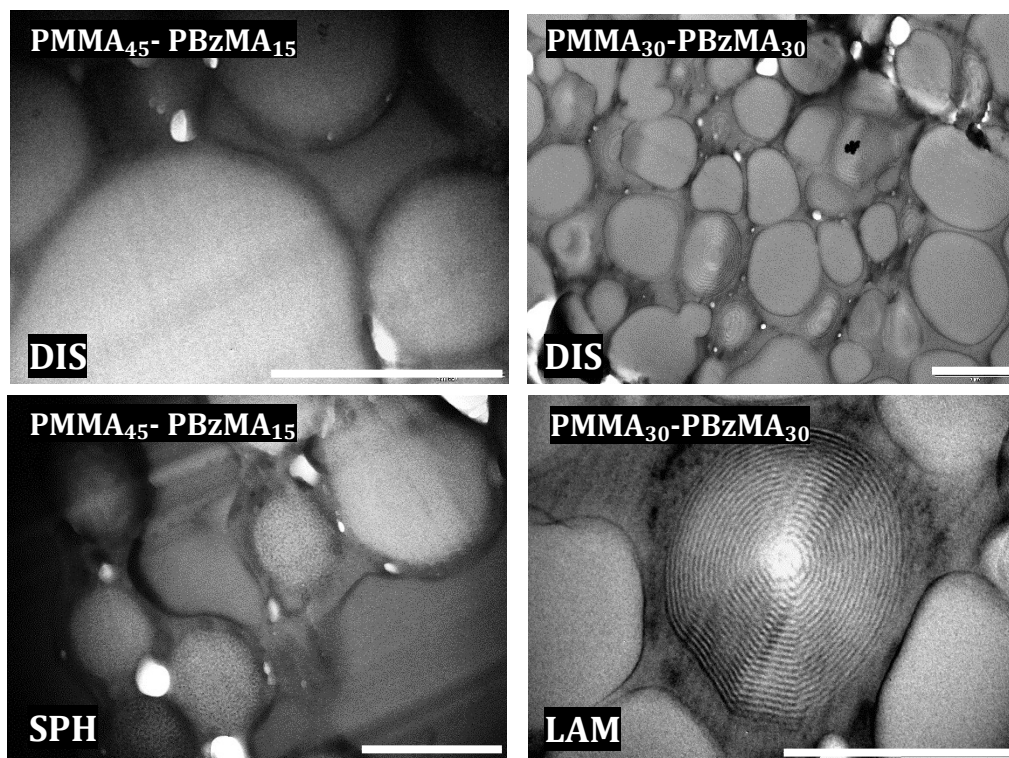
Typical polymerisation procedure: synthesis of PMMA₅₀-b-PBzMA₅₀

A high pressure autoclave (60 mL) was charged with RAFT agent (DDMAT, 0.150 mmol), AIBN (0.075 mmol), and macromonomer stabilizer (PDMS-MA, 5 wt % of total monomer mass). The autoclave was degassed by purging with CO₂ at 2 bar for 60 min, while MMA (74.8 mmol) was degassed by bubbling with argon, before being added to the autoclave. The vessel was then sealed and pressurized to 50 bar, heated to 65 °C, and the pressure topped up to 275 bar. BzMA (42.5 mmol) was degassed for 30 min and transferred to a vial containing AIBN (0.037 mmol) to be degassed for a further 10 min. The pressure in the autoclave was then reduced to <200 bar, and the monomer and initiator were added through the top of the vessel using an HPLC pump (Gilson 305). After a further 48 h of polymerization, the temperature was lowered to ambient in an ice bath, and the pressure reduced by venting the autoclave over a period of ~30 min. The total monomer loading in this polymer synthesis was 16 mL. When increasing the monomer volume fraction relative to CO₂ the above procedure was followed, and total monomer loading was increased to 25 mL, while other

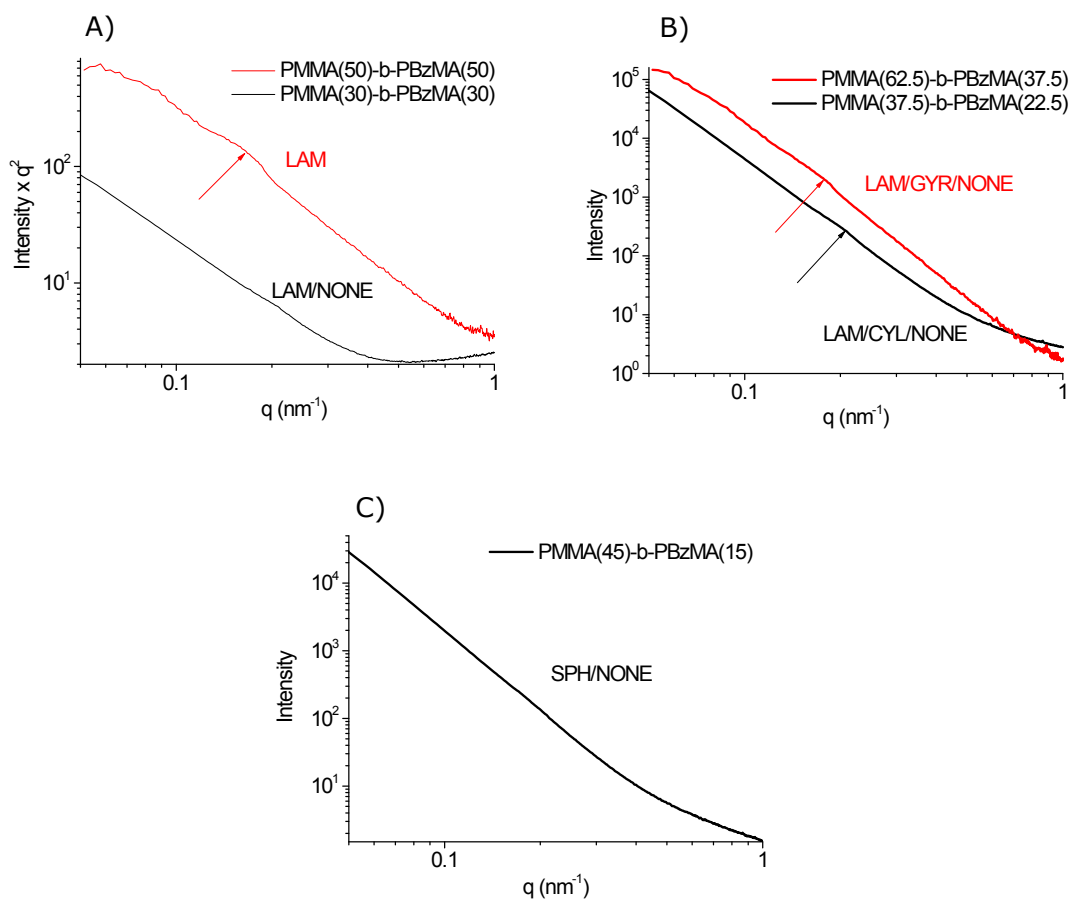
reagents were scaled accordingly. At both loadings, high monomer conversion was achieved in both steps of the polymerisation (<95%).



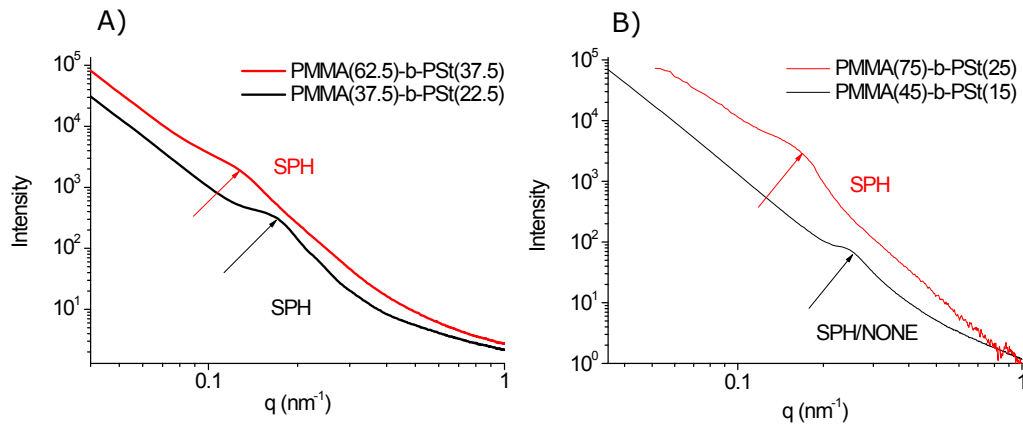
SI Figure 1: Representative GPC traces for PMMA-b-PS and PMMA-b-P4VP, demonstrating the high molecular weight shoulders due to termination by combination (solid arrow) and suspected evidence of branching (dashed arrow) that can lead to high dispersity in these polymers. The low molecular weight shoulder (*) is due to residual PDMS-MA stabiliser.



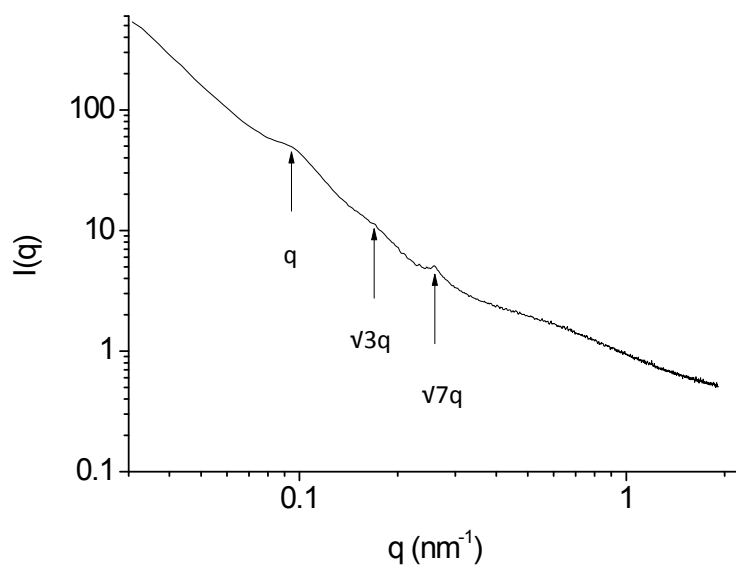
SI Figure 2: TEM images displaying the coexistence of homogeneous particles (top) with particles displaying nanoscale morphology (bottom) in different PMMA-b-PBzMA samples. The scale bar in all images is 1 μm.



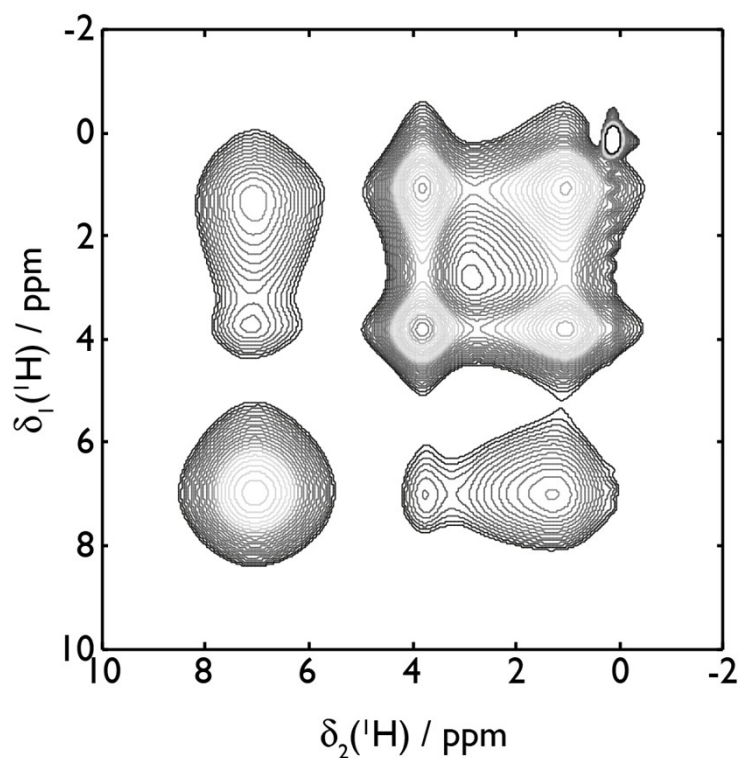
SI Figure 3: SAXS traces of various PMMA-b-PBzMA particles: (A) $w_{\text{PMMA}} \sim 0.5$, (B) $w_{\text{PMMA}} \sim 0.625$ and (C) $w_{\text{PMMA}} \sim 0.75$ at two molecular weights. The position of the Bragg reflection peak is indicated by arrow where present, and morphology observed by TEM is reported on each trace. The low peak intensity and lack of higher order peaks is due to the short range order of the morphologies within the particles. These data indicated that phase separated morphology was not persistent across all samples (for this polymer system – see SI Figure 2 above), which agreed with TEM data in some cases.



SI Figure 4: SAXS traces of various PMMA-b-PSt particles: (A) $w_{\text{PMMA}} \sim 0.625$ and (B) $w_{\text{PMMA}} \sim 0.75$. The position of the Bragg reflection peak is indicated by arrow, and morphology observed by TEM is reported on each trace. The low peak intensity and lack of higher order peaks is due to the short range order of the morphologies within the particles. These data indicated that phase separated morphology is persistent in all samples, which confirmed the TEM data.



SI Figure 5: SAXS trace from the bulk film prepared from PMMA₁₅-P4VP₄₅. The positions of the Bragg reflections at q , $\sqrt{3}q$ and $\sqrt{7}q$ confirm the cylindrical morphology observed by TEM.



SI Figure 6: Typical ^1H - ^1H spin diffusion spectrum (in this case of $\text{PMMA}_{30}\text{-PS}_{30}$ recorded with a 200 ms mixing time)

SI Table 1: PMMA-*b*-PS domain size measurements including errors from solid state NMR ^1H - ^1H spin diffusion spectra

Block Copolymer	Morphology ^a	D_{NMR} (nm)
$\text{PMMA}_{22.5}\text{-PS}_{37.5}$	LAM	24 (± 6)
$\text{PMMA}_{30}\text{-PS}_{30}$	CYL	38 (± 4)
$\text{PMMA}_{37.5}\text{-PS}_{22.5}$	SPH	33 (± 4)
$\text{PMMA}_{45}\text{-PS}_{15}$	SPH	30 (± 7)
$\text{PMMA}_{37.5}\text{-PS}_{62.5}$	LAM	50 (± 10)
$\text{PMMA}_{50}\text{-PS}_{50}$	SPH	60 (± 10)
$\text{PMMA}_{62.5}\text{-PS}_{37.5}$	SPH	41 (± 10)
$\text{PMMA}_{75}\text{-PS}_{25}$	SPH	41 (± 7)

^aDetermined by TEM imaging: LAM (lamellar), CYL (cylindrical), SPH (spherical).

References

1. J. T. Lai, D. Filla and R. Shea, *Macromolecules*, **2002**, 35, 6754-6756.